CHEMISTRY
A EUROPEAN JOURNAL

ChemPubSoc Europe

DOI: 10.1002/chem.201300955

Longitudinal Relaxation Enhancement in ^{1}H NMR Spectroscopy of Tissue Metabolites via Spectrally Selective Excitation

Noam Shemesh, Jean-Nicolas Dumez, and Lucio Frydman*[a]

Abstract: Nuclear magnetic resonance spectroscopy is governed by longitudinal (T_1) relaxation. For protein and nucleic acid experiments in solutions, it is well established that apparent T_1 values can be enhanced by selective excitation of targeted resonances. The present study explores such longitudinal relaxation enhancement (LRE) effects for molecules residing in biological tissues. The longitudinal relaxation recovery of tissue resonances positioned both down- and upfield of the water peak were measured by spectrally selective excitation/refocusing pulses, and compared with conventional water-suppressed, broadband-excited counterparts at 9.4 T. Marked LRE effects with up to threefold reductions in apparent T_1 values were observed as expected for resonances in the 6–9 ppm region; remarkably, statistically significant LRE effects were also found for several non-exchanging metabolite resonances in the 1–4 ppm region, encompassing 30–50 % decreases in apparent T_1 values. These LRE effects suggest a novel means of increasing the sensitivity of tissue-oriented experiments, and open new vistas to investigate the nature of interactions among metabolites, water and macromolecules at a molecular level.

Keywords: longitudinal relaxation enhancement · magnetic resonance spectroscopy · metabolites · neurochemistry · NMR spectroscopy

Introduction

Nuclear magnetic resonance spectroscopy (NMR, MRS) is a main modality for non-invasive studies of metabolic chemistry, in vivo.[1] In the central nervous system, ^{1}H-MRS can detect many endogenous metabolites associated with membrane synthesis (cholines (Cho)), cellular bioenergetics (creatine (Cre), lactic acid (Lac)), neurotransmission (glutamate, GABA), and other biochemical processes (taurine, inositols). Other metabolites, such as *N*-acetyl aspartate (NAA), are considered as compartment-specific viability biomarkers.[2] Monitoring changes in metabolic concentrations enables the detection of tumours,[3] the characterisation of neurodegenerative processes,[4] and studies of brain function.[5] All these MRS measurements can be deeply influenced by longitudinal (T_1) relaxation effects. Longitudinal relaxation encompasses magnetic-field dependent contributions from auto- and cross-relaxation effects, which are in turn governed by rotational correlation times involved in the molecules' dynamics.[6] Effective T_1 values can also be modified by extramolecular factors including exchanges between labile targeted protons and water,[7] or by the presence of paramagnetic agents.[8,9] Of relevance to this study is the fact that the "apparent" T_1 measured for a particular moiety, may also depend on the mode by which its NMR resonance is interrogated.[10] During the last decade numerous instances of such excitation-dependent longitudinal relaxation enhancement effects have been demonstrated in the field of biomolecular solution-state NMR spectroscopy, and have been exploited to achieve substantial improvements in the signal-to-noise ratio (SNR) achievable per unit time in protein and nucleic acid NMR experiments.[10–12] The ensuing approaches rely on targeting resonances with spectrally selective pulses; the abundant reservoir of magnetically unperturbed water and macromolecular ^{1}Hs can then act as relaxation "sinks", replenishing the depleted polarisation by chemical exchange and/or cross-relaxation with the excited macromolecular resonances.[11–13] Such longitudinal relaxation enhancement (LRE) effects afford the opportunity to reduce the NMR recycling delays,[10–12] as well as to interrogate interesting aspects of macromolecular folding and flexibility.[14] Furthermore, if multidimensional acquisitions are involved where sampling rather than sensitivity considerations define the rate-determining step, significant acceleration factors can be achieved by such selective excitations. This has facilitated high-resolution studies of biochemical dynamics,[10–12,14–18] including real-time studies of protein and nucleic acid folding processes and binding dynamics of small molecules in proteins.[19,20]

Although these relaxation-enhancing concepts are having a decisive impact in in vitro biophysical NMR spectroscopy, their influence in tissue-oriented MRS remains to be fully assessed. Clearly, numerous differences distinguish NMR in protein solutions from MRS in biological tissues. Still, a number of analogies can be made, including the coexistence in both systems of resonances of interest with a large water reservoir; correlation times that for many metabolites and/or tissue-originating signatures can be reasonably hypothesised to be different from those in free solutions;[21] and in-

[a] Dr. N. Shemesh, Dr. J.-N. Dumez, Prof. L. Frydman
Department of Chemical Physics, Weizmann Institute of Science
Rehovot 76100 (Israel)
E-mail: lucio.frydman@weizmann.ac.il

herent sensitivity problems of tissue MRS that parallel their in vitro biomolecular counterparts. The existence of mutual magnetisation exchanges between water and labile tissue protons resonating downfield of the water peak is in fact well known, and constitutes the basis of chemical exchange saturation transfer (CEST)[22] and magnetisation transfer (MT)[23] experiments. A magnetic coupling between water and labile tissue protons was further evidenced upon by using water "flip-back" modules:[24–26] pH-dependent changes in the labile protons' signal intensities are then directly observed.[25] On the other hand, the occurrence of spontaneous polarisation transfers between water and non-labile metabolic resonances resonating *upfield* from H_2O are much less obvious. Sole evidences for these effects stems from slight changes in the appearances of metabolic tissue signals upon applying a selective water inversion;[27–29] when using different water suppression schemes;[30] or when off-resonance saturation is employed.[31,32] These changes in upfield metabolic signal were mostly interpreted as NOE contributions from the water resonance or as polarisation transfer processes involving free metabolites and immobilised metabolite pools.[23,27]

This study quantitatively examines LRE effects for labile and non-labile resonances in biological tissues. To this end we utilise selective excitation schemes that can explore the potential existence of LRE effects, and eventually harness them for enhancing the quality of MRS spectra. Although metabolic T_1 values have been measured in high magnetic fields,[33,34] relaxation enhancement effects have, to our knowledge, not been directly interrogated by apparent T_1 measurements. In this study, we quantify the changes in the apparent longitudinal relaxation T_1 values for both exchanging (H_2O-downfield) and for non-labile (H_2O-upfield) protons, upon switching from broadband to selective excitation methods. We find, as expected, strong LRE effects for the downfield resonances; surprisingly, *we also find statistically significant reductions in apparent T_1 for non-labile methyl peaks resonating upfield of water.* The potential nature of these effects is briefly discussed, and their use for enhancing the sensitivity of ^{1}H MRS of tissues is explored and demonstrated.

Results and Discussion

A prerequisite for observing longitudinal relaxation enhancement effects for a given family of resonances of interest, involves keeping a majority of ^{1}H magnetisation unperturbed. Preserving all but the targeted magnetisations aligned along the z axis was here achieved by combining spectrally selective excitation with spectrally selective refocusing pulses, all of them designed by the Shinnar–Le Roux (SLR) algorithm.[35] The designed pulse and its ensuing frequency domain response profile over the course of the experiment are presented in Figure 1 A and B, respectively. Note that the water resonance at about 4.7 ppm is completely avoided. On the other hand, the pulse duration required

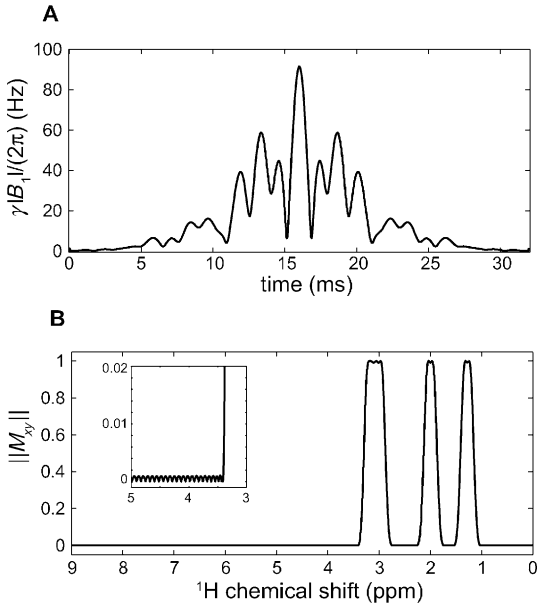

Figure 1. A) Example of the 32 ms multiband linear-phase equiripple pulse used to excite the H_2O-upfield resonances in this study. B) Transverse magnetisation profile elicited in the frequency domain, showing that Lac (lactic acid), NAA (*N*-acetyl aspartate), Cre (creatine) and Cho (cholines; 1.33, 2.02, 3.05 and 3.25 ppm, respectively) are uniformly excited, whereas the water resonance is avoided, in accordance with the close-up shown in the inset. Experiments showed that the water resonance was not excited by these pulses by more than 10^{-4} of its full intensity. The Lac and NAA bandwidths were 120 Hz (0.3 ppm) each, whereas the Cre and Cho resonances were excited with a joint 200 Hz (0.5 ppm) band centred at 3.1 ppm.

for such high-definition stop-bands is rather long, rendering the ensuing signal vulnerable to large offset-dependent phase distortions. Therefore, a single-band refocusing pulse flanked by two weak crusher gradients was inserted to compensate for the significant chemical shift evolution otherwise accrued for different resonances. The ensuing spin echo sequence is hereafter denoted as the LRE sequence (Figure 2 A):

$$90^\circ_{SLR}-\tau_a-G_c-180^\circ_{SLR}-G_c-\tau_b-\text{acq.}-\text{r.d.} \quad (1)$$

where G_c denotes small crusher gradients of duration δ, $\tau_a = (TE/2-\tau_{90}/2-\delta-\tau_{180}/2)$ and $\tau_b=(\tau_a+\tau_{90}/2)$ are delays given by the excitation pulse duration τ_{90}, the refocusing pulse duration τ_{180}, and the total echo time (TE), acq. denotes a signal acquisition of duration A_t, and r.d. is a recycling delay. As a control sequence, we used the water-suppressed WATERGATE (WG) sequence[36] (Figure 2 B), in which a broad spectrum of resonances is affected by the broadband pulses. This includes water molecules that are excited in the beginning of the sequence and eventually crushed by gradients such that ideally, the bulk magnetisation is zero. This is in contrast with LRE, in which ideally the longitudinal component of the water magnetisation is left unperturbed, that is, $M_z=M_0$. Also assayed was a sequence incorporating a chemical shift selective[37] (CHESS) water-suppression module prior to the LRE sequence (CHESS-LRE, Fig-

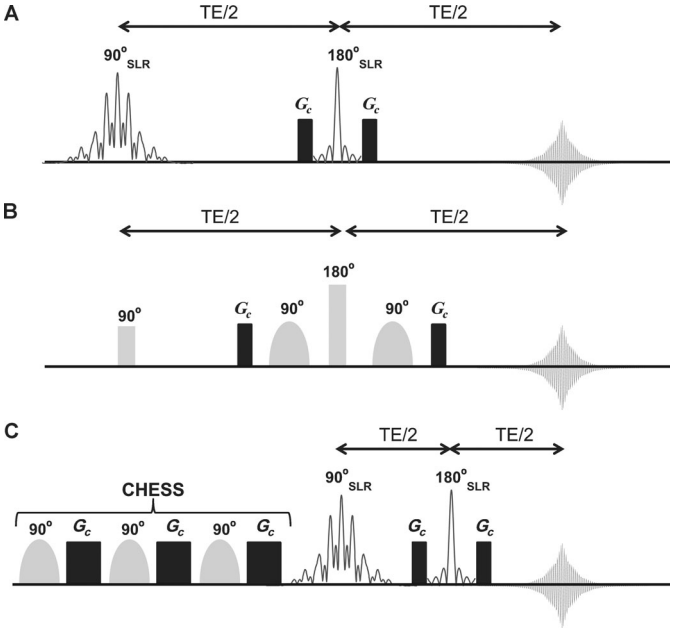

Figure 2. Description of the spin-echo sequences used in this study. A) LRE sequence, designed to selectively excite and refocus resonances of interest whilst avoiding excitation/inversion of the water resonance. The selective excitation and refocusing pulses are shown in blue and denoted $90°_{SLR}$ and $180°_{SLR}$, respectively, G_c denotes small crushers. The first pulse was phase cycled through two steps of 0 and 180°, together with the receiver. B) WATERGATE (WG) sequence,[36] employing broadband excitation followed by water-selective pulses and gradients designed to actively crush the water resonance. C) CHESS-LRE,[37] employing water-selective excitation pulses and crushers prior to the LRE sequence, which then excites and refocuses only the resonances of interest. Note that unlike WG, CHESS-LRE avoids broadband excitation. RF pulses are shown in grey and crusher gradients are shown in black; hard pulses are represented by rectangles and soft, water-selective pulses are represented by oval shapes.

ure 2C); this sequence avoids the broadband excitation inherent to WG, yet still relies on crushing the water peak.

Figure 3A compares representative spectra arising from LRE and WG sequences in a sample mouse brain for a spectral region lying downfield of water. Although not all of these resonances have been assigned, this 6–11 ppm region is mainly comprised from labile protons. The LRE spectrum of this region at $TE = 40$ ms is of high quality and exhibits no phasing complications or discernible water resonance (Figure 3A, blue). This enables a robust quantification of the effective T_1 values for all the downfield resonances by using the progressive saturation[38] (PS) technique. The WG spectrum by contrast shows lower peak intensities, worse SNR, and a strong residual water peak (Figure 3A, red); upon using the WG scheme only the longitudinal recoveries of the peaks marked as "a" and "b" (defined in Figure 3A) could be quantified. For these peaks, the recovery times revealed by the LRE sequence were short: 0.82(±0.03) and 0.74(±0.06) s, respectively; these effective T_1 values became 2.39(±0.52) and 2.03±(0.18) s upon WG examination (see Table 1 for further results). The nearly 300% differences in effective T_1 values evidenced by these measurements are indicative of a longitudinal relaxation enhancement, driven by

Table 1. Apparent T_1 relaxation times obtained by progressive saturation upon using the LRE and the WG sequences.[a]

Metabolite	Apparent T_1 [s] ±S.D. by LRE	Apparent T_1 [s] ±S.D. by WG
peak "a"	0.74±0.06	2.03±0.18
peak "b"	0.82±0.03	2.39±0.52
peak "c"	0.57±0.09	N/A
peak "d"	0.81±0.09	N/A
Lac[b]	1.05±0.07	1.56±0.05
NAA	1.30±0.06	1.52±0.26
Cre[c]	1.20±0.07	1.71±0.04
Cho[d]	1.33±0.10	1.78±0.08

[a] Upper four rows: T_1 relaxation values for the down-field resonances "a–d", defined in Figure 3a. Lower four rows: apparent T_1 relaxation values and statistical analysis for upfield metabolites ($N = 4$ brains). Statistical significance: [b] $p < 0.003$, [c] $p < 0.0004$, [d] $p < 0.01$. N/A = Not available.

chemical exchange with water and/or by cross-relaxation. This behaviour reflects in fact an "inverse" of the CEST experiment, in which saturation of the downfield region is relayed to the water resonance by chemical exchange.[22,23] The LRE observed for these downfield resonances is also analogous to what is observed for N–H proton resonances in protein solutions, in which the corresponding peaks are also subject to strong changes in their apparent T_1 times upon selective excitation.[10,11,14] To ensure that the LRE effects are not sequence-specific, we also obtained spectra with the LRE sequence preceded by a CHESS water-suppression module (Figure 3B). The same trends as reported above for WG were then observed for the downfield resonances.

Whereas LREs could be expected for the downfield region given the involvement of labile amide resonances, the fact that also small metabolite resonances resonating upfield of water evidence relaxation enhancement, is more surprising. To illustrate this hitherto unreported effect, we centre on the methyl ^{1}Hs of Lac, NAA, Cre and Cho. A multiband selective excitation pulse like the one described in Figure 1 was applied on these resonances; Figure 3C compares representative LRE and WG spectra of these methyl groups in tissues for $TE = 144$ ms (chosen to produce a completely inverted Lac signal due to J-coupling in the WG spectrum). The peaks of interest are excited with good sensitivity by the LRE sequence, with complete cancellation of the water resonance and excellent baseline/phasing spectral characteristics (Figure 3C). Another remarkable feature of the LRE spectrum is that the Lac signal is in-phase despite our choice of $TE = 1/J$; this is a consequence of the spectrally selective $180°_{SLR}$ pulse, which does not refocus the coupling partner of the Lac 1.33 ppm resonance. To establish a more comprehensive comparison, CHESS-LRE measurements were also performed on a different brain (Figure 3D). The enhanced SNR of LRE versus the CHESS-LRE is already an indication that relaxation enhancements occur even in the upfield region. Representative stacked plots of such experiments are shown in Figure 4, and demonstrate the robustness of the raw data in these experiments.

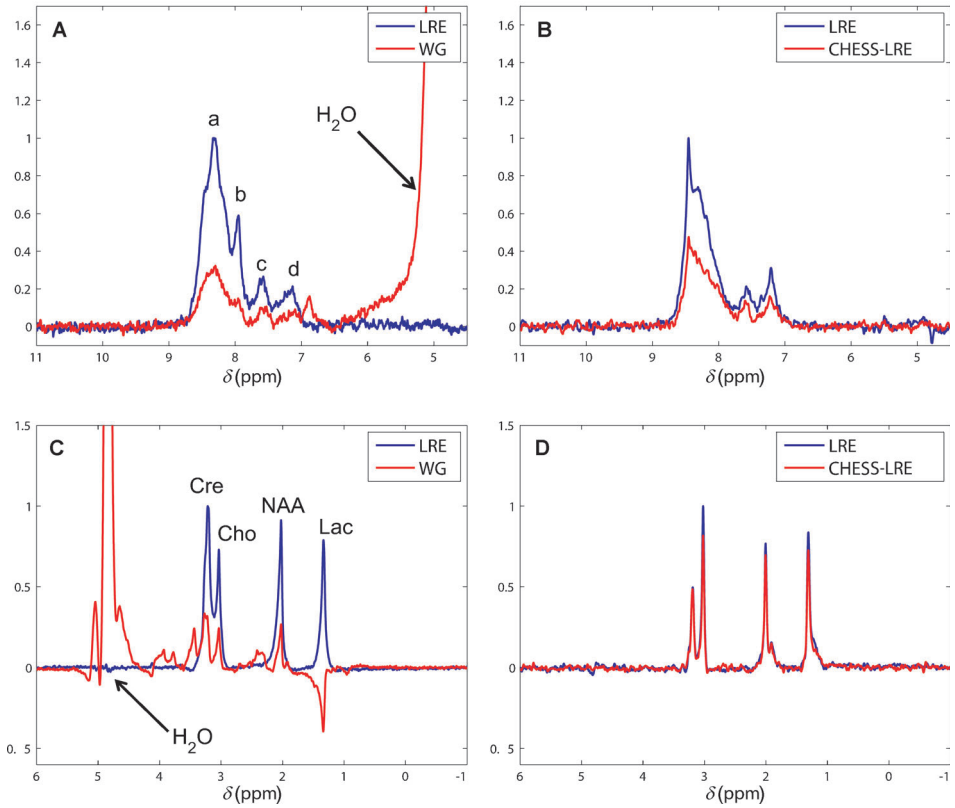

Figure 3. Representative spectra supporting the relaxation measurements reported in this study for: A), B) downfield ($TE = 40$ ms), and C), D) upfield ($TE = 144$ ms) regions of excised mouse brains. A), C) Direct comparisons of LRE and WG in a single brain, and B), D) direct comparisons of LRE and CHESS-LRE in another sample brain. Note that upon using LRE the water resonance is completely avoided, whereas resonances of interest are excited with high sensitivity. For LRE in the downfield region, a single-band 32 ms excitation pulse was used (BW = 3 ppm centred around 8.5 ppm) as well as a single-band 4 ms refocusing pulse (BW = 10 ppm, shifted 6.7 ppm upfield from the on-resonant water). For LRE in the upfield region, a 32 ms multiband excitation pulse was used (Figure 1). The same spectrally selective refocusing pulse was used as in the downfield experiment, apart from its carrier being shifted 6.2 ppm upfield of water. Vertical scales are shown in a common arbitrary unit scale in each panel.

To further quantify LRE effects, apparent T_1 values were extracted from these datasets. Figure 5 summarises these T_1 measurements for the Lac, NAA, Cre and Cho resonances in ex vivo brains, comparing the water-suppressed, broadband excited signal originating from WG (red circles) with the LRE counterparts (black squares); also shown are measurements conducted with the CHESS-LRE sequence (blue triangles). Even a superficial appraisal indicates shorter apparent T_1 relaxation times for all metabolites upon using a LRE sequence, over counterparts measured with a WG-based one.

To further quantify these T_1 effects, four different brains were extracted, and the T_1 values obtained from LRE and WG were subsequently analysed by using a paired t-test. These results are summarised in Table 1 (bottom rows) and in Figure 6. Statistically significant changes were evidenced for Lac, Cre and Cho, for which apparent T_1 values measured by LRE were approximately 30–50% shorter than those measured by the WG sequence, which employs broadband RF pulses. The Lac resonance showed the most dramatic decrease (nearly 50% in apparent T_1), whereas decreases of approximately 40 and 34% were measured for the Cre and Cho resonances, respectively (Table 1). Interestingly, the NAA resonance failed to reach a statistically significant threshold to establish relaxation enhancement. Furthermore, when apparent T_1 values obtained from LRE were compared to CHESS-LRE (Figure 5), NAA also showed negligible differences in apparent T_1. Interestingly, NAA is considered as compartmentalised in the intra-axonal space;[2] thus, the differential effects shown above may reflect on the involvement of other resonances in the LRE phenomenon, which are excited by the broadband WG pulses but not in the highly selective CHESS-LRE. We note in passing that these effects were not confined to mouse brains: similar trends were also found for fresh ex vivo pig spinal cords (data not shown). By contrast, as expected for small molecules having short correlation times in solution, no distinctions in apparent T_1 between LRE/WG were evidenced for any resonance in substances chosen for a "metabolic aqueous phantom" (Figure 7). This demonstrates that the LRE effects originate from an interaction of the metabolites with water within the host tissue.

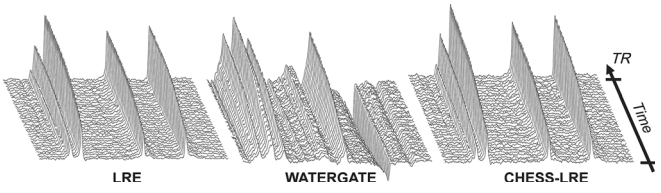

Figure 4. Stacked plots for a typical progressive-saturation experiment designed to measure the metabolites' apparent T_1 values for LRE, WG, and CHESS-LRE methods. These data are representative for all mouse brains used in this study. Although the SNR of LRE and CHESS-LRE are higher, robust quantification of T_1 is possible for all methods.

The apparent T_1 modifications quantified here, particularly the changes observed in the 1–4 ppm region, offer insights into the interactions between small metabolites and their host tissues. As in their biomolecular NMR counterparts, they also suggest that these effects can be harnessed to enhance MRS spectra in tissues. From a fundamental point of view, the apparent T_1 relaxation enhancement observed

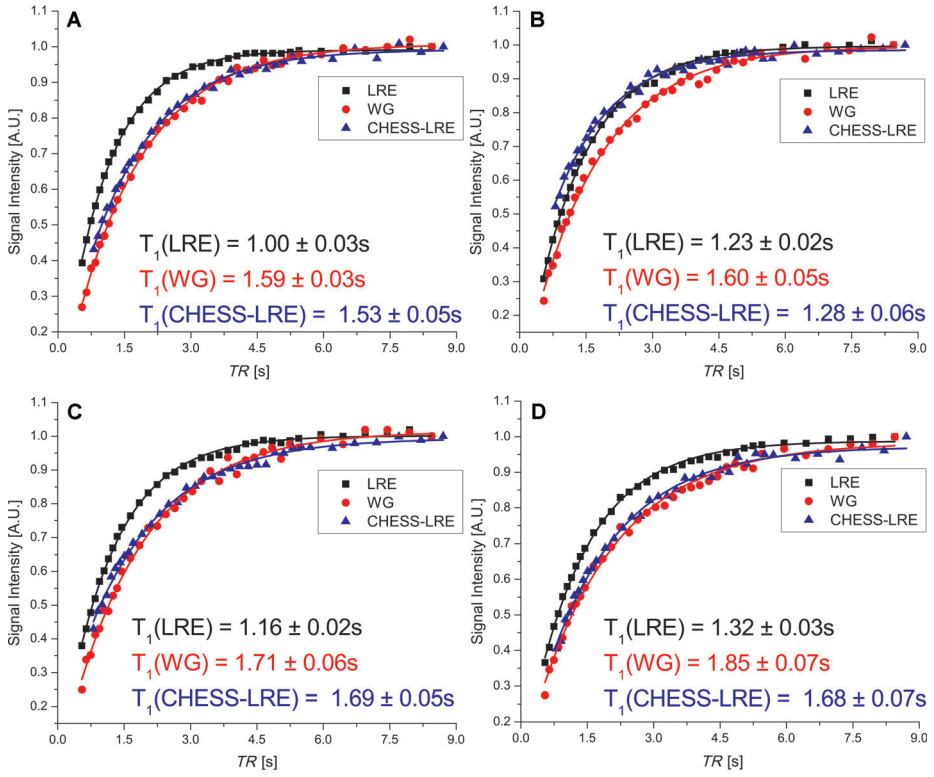

Figure 5. Representative longitudinal relaxation build-up curves for LRE (black) WG, (red) and CHESS-LRE (blue) sequences for: A) Lac, B) NAA, C) Cre, and D) Cho in the mouse brain. The data were normalised to the last *TR* point for display purposes and the indicated apparent T_1 values correspond to the fits in the solid curves.

upon selectively exciting metabolic resonances, suggests a number of extramolecular cross-relaxation effects. These are likely to involve interactions between metabolites and immobile proton pools, including immobilised enzymes and/or protein complexes, and metabolites bound to hydrophobic macromolecules. Particularly worthy of identification is the role played by non-aqueous magnetisation sources, as well as by dispersions of the metabolites' chemical shifts at binding sites, in this relaxation enhancement behaviour. Further studies will be needed to establish the direct mechanisms mediating these effects, and to clarify whether they arise from chemical exchanges or polarisation transfer interactions. These experimental clarifications could open valuable vistas towards investigating the nature of metabolic interactions in tissues—among the small molecules themselves, with the backbone of macromolecules, and with the ubiquitous water. Further, the fact that different metabolites undergo distinct relaxation enhancements also suggests that these LRE effects may become a source of contrast for both normal as well as diseased tissues. Notice as well that the LRE measurements as hereby carried out were biased towards long-T_2 species, and that in addition to manipulating the targeted methyl groups, the sequences assayed perturbed significant portions of the macromolecular tissue protons. It is conceivable that even stronger relaxation enhancement effects will arise once these limitations are lifted. Finally, we note that the LRE approach further enhances the obtained spectra by obviating the need for active water-suppression—albeit at the expense of longer TEs dictated from the rather long RF pulses required for exquisite spectral specificity.

Conclusion

Significant longitudinal relaxation enhancement effects were observed upon selective excitation in CNS tissue for both exchanging resonances downfield of water as well as non-exchanging methyl resonances upfield of water. From a methodological perspective, these findings suggest that the sensitivity of MRS experiments can be enhanced by effectively "decreasing" the apparent T_1 values by selective excitation. This could result in higher SNR per unit time, particularly at higher magnetic fields, and lead to new approaches combining selective RF pulses with Ernst-angle excitations that enable an optimal signal averaging.[12,38] This could also be put to good advantage for speeding up the acquisition of certain 2D MRS spectra in vivo, and/or high-dimensional spectroscopic images. Further advantages of these sequences result from their avoidance of active water suppression, leading to high fidelity spectra with no baseline distortions. The LRE approach can be also useful for localised MRS experiments, especially since localisation modules can be inserted into the sequence (e.g., by using double spin echoes, which do not perturb the longitudinal water magnetisation[39]), or for *J*-editing by the spectral profile of the 180° refocusing pulse. These modules can also be used as templates for other sequences probing different metabolic properties, such as diffusion coefficients,[40] or micro-architectural environments.[41] Also worth noting is that in many studies, quantification of metabolites relies on the assumption that T_1 is known.[42] Since as shown here the apparent T_1 depends on the mode of excitation, these effects imply that particular attention needs to be placed for metabolite quantification. The implication of these various features is currently being investigated under in vivo conditions.

Experimental Section

All experiments were performed on a Bruker Avance 9.4 T vertical bore scanner, using a micro5 imaging probe capable of producing pulsed mag-

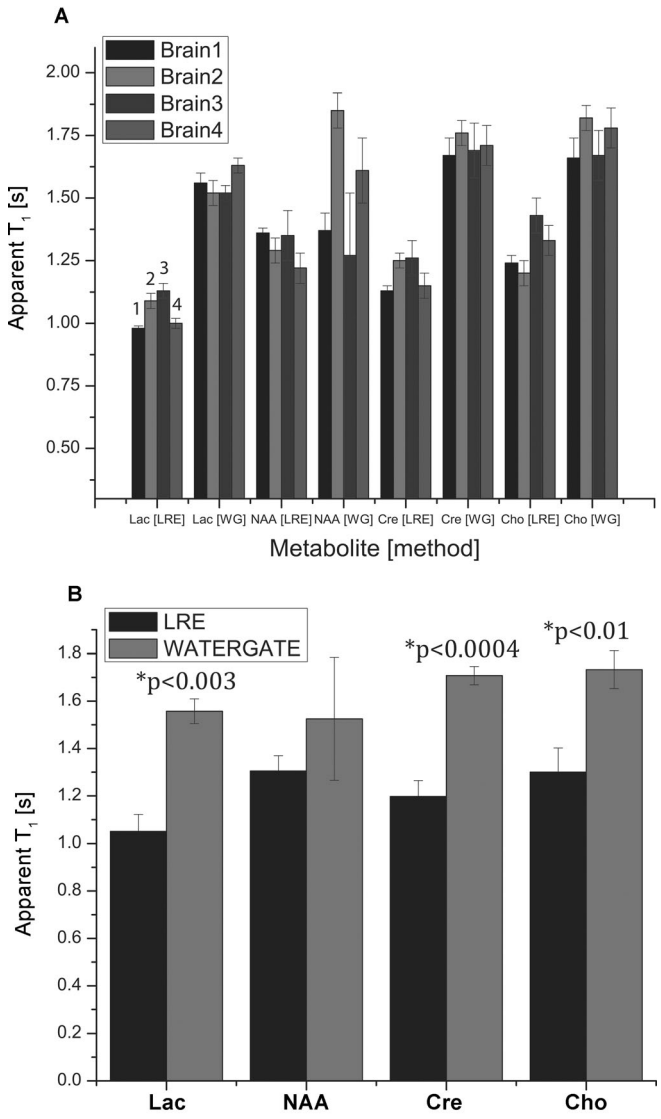

Figure 6. A) Raw data, and B) statistical analysis of apparent T_1 values measured for the four sample mouse brains investigated. A) The apparent T_1 values obtained from each brain, including the confidence limits of every fit. The only exception to a consistent value of the apparent T_1 values arises from the NAA WG measurements, which appear to fluctuate more than the T_1 values of other metabolites. For ease of interpretation of the bar plots, brain identification numbers are clearly marked on the first four bars. B) The mean apparent T_1 values and their standard deviations, together with the ensuing t-tests, reveal statistically significant T_1 reductions for Lac, Cre, and Cho but not NAA.

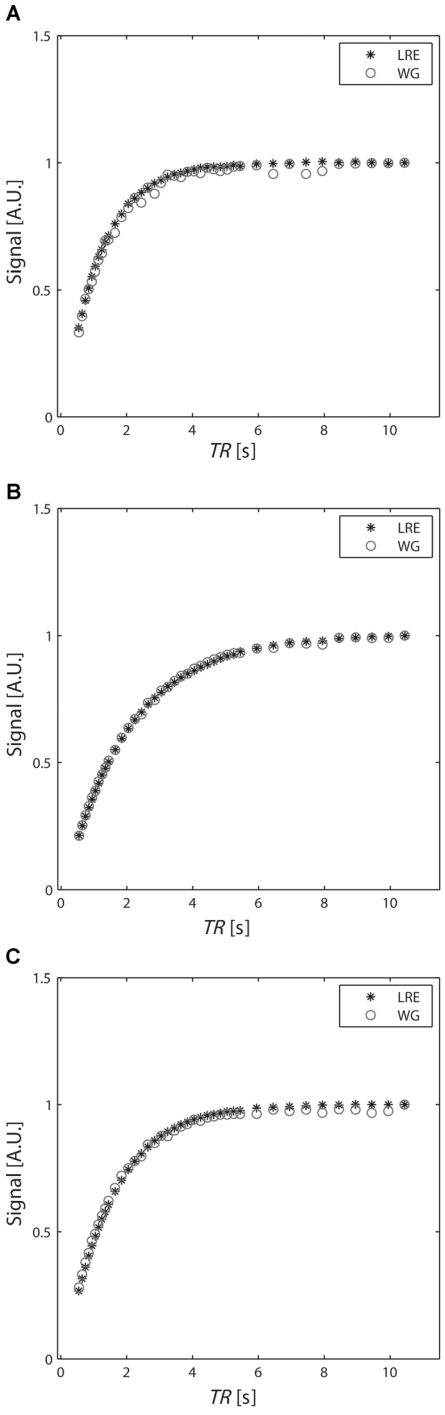

Figure 7. Effective T_1 build-up curves obtained upon using LRE and WG sequences for: A) MeOH, B) acetone, and C) *t*BuOH in resonances of a phantom comprising a mixture of the three substances in water (slightly doped with $CuSO_4$). Despite the fact that these small molecules vary in molecular size and of their inclusion of exchanging hydroxyl groups, the WG and LRE methodologies give identical T_1 build-up curves upon progressive saturation, unlike the results obtained in the biological tissues.

netic field gradients of 2880 $mT\,m^{-1}$ in all three directions. Targeted in this study were fresh mouse brains washed briefly with PBS after their extraction and inserted immediately thereafter into a 10 mm NMR tube filled with Fluorinert. Care was taken to ensure the structural integrity of these samples, which were allowed to thermally equilibrate in the magnet for about 30 min prior to data acquisition. Line widths of 15–30 Hz were routinely obtained for all specimens. The entire measurement on each brain was concluded in less than 50 min to ensure minimal tissue deterioration; this was further ascertained by comparing spectra at the beginning and end of the experiments. Animal protocols and maintenance were done in accord with the guidelines of the Committee on Animals of the Weizmann Institute of Science.

The LRE sequence shown in Figure 2A consists of a selective excitation pulse, designed through the SLR algorithm[35] to excite only the resonance of interest, and a refocusing pulse for refocusing the chemical shift offsets accrued during the excitation pulse. Special care was taken upon designing the SLR-based pulses to keep water's magnetisation unper-

turbed along the z axis at all times; this proved more efficient than relying on broadband excitations followed by customised flip-back pulses. Weak gradient pulses were applied on either side of the refocusing pulse to crush residual unwanted magnetisation. For selective excitation of the upfield resonances of interest (Lac, NAA, Cre and Cho) a 32 ms multiband excitation pulse was used, encompassing three bands centred around 1.33, 2.02 and 3.1 ppm, with bandwidths of 120, 120 and 200 Hz (0.3, 0.3 and 0.5 ppm), respectively. For selective excitation of downfield resonances, a single-band 32 ms pulse with a bandwidth 3 ppm was centred around 8.5 ppm. For selective refocusing, we designed a 4 ms 180° pulse with a bandwidth 10 ppm, which was shifted 6.2 ppm upfield from the on-resonant water for experiments targeting upfield resonances and 6.7 ppm downfield from water for experiments targeting downfield resonances.

To measure T_1 values with water-suppression, we used the WATERGATE sequence[36] shown in Figure 2B. In such sequences the initial 90° pulse is broadband; the water magnetisation is then crushed by the selective pulses and gradients, leading ideally to a null H_2O magnetisation at the beginning of the signal acquisition. Another water-suppressed sequence that was used was the CHESS-LRE (Figure 2C) sequence, in which a CHESS water-suppression module[37] was added just prior to the LRE sequence; this sequence avoids broadband excitation, and targets the sole excitation of the water resonance and the resonances of interest.

As a robust route for comparing the apparent T_1 values observed with the LRE, the WG, and the CHESS-LRE pulse sequences, the progressive saturation (PS) technique was used.[38] This entailed preparing steady-state magnetisations by applying a sufficient number of "dummy" scans (DS) and then collecting spectra at various repetition times, TRs, where $TR = TE + A_t +$ r.d. These PS experiments were conducted for both sequences with 36 points ranging from $0.544\ \mathrm{s} \leq TR \leq 8.544\ \mathrm{s}$, and apparent T_1 values were extracted from a fit of these data to $M(TR) = M_0(1-\exp(-TR/T_1))$. For all experiments in this study, DS = 8 and the number of averaged scans was four. Experiments were performed on four different mouse brains and the T_1 values extracted for the different metabolites from WG and LRE were statistically compared by a paired t-test. Identical PS experiments were conducted on a metabolite "phantom" comprising of approximately 50 mM tBuOH, MeOH and acetone in an aqueous solution slightly doped with $CuSO_4$.

Acknowledgements

The authors thank Dr. Nava Nevo (Weizmann Veterinary Services) for assistance with the brain specimens. This work was supported by the Marie Curie Action ITN METAFLUX (project 264780), ERC Advanced Grant 246754, a Helen and Martin Kimmel Award for Innovative Investigation, and the generosity of the Perlman Family Foundation.

[1] R. A. de Graaf, *In-Vivo NMR Spectroscopy: Principles and Techniques*, 2nd ed., Wiley, Chichester, **2007**.
[2] J. R. Moffett, B. Ross, P. Arun, C. N. Madhavarao, A. M. A. Namboodiri, *Prog. Neurobiol.* **2007**, *81*, 89–131.
[3] C. Choi, S. K. Ganji, R. J. Deberardinis, K. J. Hatanpaa, D. Rakheja, Z. Kovacs, X. L. Yang, T. Mashimo, J. M. Raisanen, I. Marin-Valencia, J. M. Pascual, C. J. Madden, B. E. Mickey, C. R. Malloy, R. M. Bachoo, E. A. Maher, *Nat. Med.* **2012**, *18*, 624–629.
[4] C. Demougeot, P. Garnier, C. Mossiat, N. Bertrand, M. Giroud, A. Beley, C. Marie, *J. Neurochem.* **2001**, *77*, 408–415.
[5] Y. Lin, M. C. Stephenson, L. J. Xin, A. Napolitano, P. G. Morris, *J. Cereb. Blood Flow Metab.* **2012**, *32*, 1484–1495.
[6] D. Neuhaus, M. P. Williamson, *The Nuclear Overhauser Effect in Structural and Conformational Analysis*, 2nd ed., VCH, Weinheim, **1992**.
[7] G. Otting, E. Liepinsh, K. Wuthrich, *Science* **1991**, *254*, 974–980.
[8] S. Cai, C. Seu, Z. Kovacs, A. D. Sherry, Y. Chen, *J. Am. Chem. Soc.* **2006**, *128*, 13474–13478.
[9] T. Madl, W. Bermel, K. Zangger, *Angew. Chem.* **2009**, *121*, 8409–8412; *Angew. Chem. Int. Ed.* **2009**, *48*, 8259–8262.
[10] P. Schanda, B. Brutscher, *J. Am. Chem. Soc.* **2005**, *127*, 8014–8015.
[11] P. Schanda, H. Van Melckebeke, B. Brutscher, *J. Am. Chem. Soc.* **2006**, *128*, 9042–9043.
[12] P. Schanda, *Prog. Nucl. Magn. Reson. Spectrosc.* **2009**, *55*, 238–265.
[13] K. Pervushin, B. Vogeli, A. Eletsky, *J. Am. Chem. Soc.* **2002**, *124*, 12898–12902.
[14] E. Rennella, T. Cutuil, P. Schanda, I. Ayala, V. Forge, B. Brutscher, *J. Am. Chem. Soc.* **2012**, *134*, 8066–8069.
[15] S. Bruschweiler, P. Schanda, K. Kloiber, B. Brutscher, G. Kontaxis, R. Konrat, M. Tollinger, *J. Am. Chem. Soc.* **2009**, *131*, 3063–3068.
[16] M. Gal, P. Schanda, B. Brutscher, L. Frydman, *J. Am. Chem. Soc.* **2007**, *129*, 1372–1377.
[17] C. Arnero, P. Schanda, M. A. Dura, I. Ayala, D. Marion, B. Franzetti, B. Brutscher, J. Boisbouvier, *J. Am. Chem. Soc.* **2009**, *131*, 3448–3449.
[18] B. Brutscher, J. Boisbouvier, A. Pardi, D. Marion, J. P. Simorre, *J. Am. Chem. Soc.* **1998**, *120*, 11845–11851.
[19] M. Gal, M. K. Lee, G. Varani, L. Frydman, *Proc. Natl. Acad. Sci. USA* **2010**, *107*, 9192–9197.
[20] M. Quinternet, J. P. Starck, M. A. Delsuc, B. Kieffer, *Chem. Eur. J.* **2012**, *18*, 3969–3974.
[21] P. A. Bottomley, T. H. Foster, R. E. Argersinger, L. M. Pfeifer, *Med. Phys.* **1984**, *11*, 425–448.
[22] J. Y. Zhou, P. C. M. Van Zijl, *Prog. Nucl. Magn. Reson. Spectrosc.* **2006**, *48*, 109–136.
[23] D. Leibfritz, W. Dreher, *NMR Biomed.* **2001**, *14*, 65–76.
[24] S. Mori, C. Abeygunawardana, M. O. Johnson, P. C. M. Van Zijl, *J. Magn. Reson. Ser. B* **1995**, *108*, 94–98.
[25] S. Mori, S. M. Eleff, U. Pilatus, N. Mori, P. C. M. Van Zijl, *Magn. Reson. Med.* **1998**, *40*, 36–42.
[26] P. C. M. Van Zijl, J. Zhou, N. Mori, J. F. Payen, D. Wilson, S. Mori, *Magn. Reson. Med.* **2003**, *49*, 440–449.
[27] M. J. Kruiskamp, R. A. de Graaf, G. van Vliet, K. Nicolay, *Magn. Reson. Med.* **1999**, *42*, 665–672.
[28] M. J. Kruiskamp, R. A. de Graaf, J. van der Grond, R. Lamerichs, K. Nicolay, *NMR Biomed.* **2001**, *14*, 1–4.
[29] E. L. MacMillan, D. G. Q. Chong, W. Dreher, A. Henning, C. Boesch, R. Kreis, *Magn. Reson. Med.* **2011**, *65*, 1239–1246.
[30] E. L. MacMillan, C. Boesch, R. Kreis, *Magn. Reson. Med.* **2012**; DOI: 10.1002/mrm.24537.
[31] R. A. de Graaf, A. van Kranenburg, K. Nicolay, *Magn. Reson. Med.* **1999**, *41*, 1136–1144.
[32] G. Helms, J. Frahm, *NMR Biomed.* **1999**, *12*, 490–494.
[33] C. Cudalbu, V. Mlynarik, L. J. Xin, R. Gruetter, *Magn. Reson. Med.* **2009**, *62*, 862–867.
[34] R. A. de Graaf, P. B. Brown, S. McIntyre, T. W. Nixon, K. L. Behar, D. L. Rothman, *Magn. Reson. Med.* **2006**, *56*, 386–394.
[35] J. Pauly, P. Leroux, D. Nishimura, A. Macovski, *IEEE Trans. Med. Imaging* **1991**, *10*, 53–65.
[36] M. Piotto, V. Saudek, V. Sklenar, *J. Biomol. NMR* **1992**, *2*, 661–665.
[37] A. Haase, J. Frahm, W. Hanicke, D. Matthaei, *Phys. Med. Biol.* **1985**, *30*, 341–344.
[38] R. Freeman, H. D. W. Hill, *J. Chem. Phys.* **1971**, *54*, 3377, 1–11.
[39] A. Tannús, M. Garwood, *NMR Biomed.* **1997**, *10*, 423–434.
[40] E. T. Wood, I. Ronen, A. Techawiboonwong, C. K. Jones, P. B. Barker, P. Calabresi, D. Harrison, D. S. Reich, *J. Neurosci.* **2012**, *32*, 6665–6669.
[41] N. Shemesh, T. Adiri, Y. Cohen, *J. Am. Chem. Soc.* **2011**, *133*, 6028–6035.
[42] V. Mlynárik, C. Cudalbu, L. J. Xin, R. Gruetter, *J. Magn. Reson.* **2008**, *194*, 163–168.

Received: March 13, 2013
Published online: September 3, 2013

